# Catalog and Description of GPS and WAAS L1 C/A Signal Deformation Events

Karl W. Shallberg, Swen D. Ericson, *Zeta Associates*
Eric Phelts, Todd Walter, *Stanford University*
Karl Kovach, *The Aerospace Corporation*
Eric Altshuler, *Sequoia Research Corporation*

## BIOGRAPHIES

Mr. Karl W. Shallberg is a Senior Associate with Zeta Associates Inc. and currently is working GPS receiver performance and system engineering issues for the FAA GNSS Program. He previously was president of Grass Roots Enterprises Inc. and worked for the U.S. Government. He received his B.S. in physics from Norwich University.

Mr. Swen D. Ericson has been involved with GPS and WAAS system engineering for the FAA at Zeta Associates since 2003. Prior to joining Zeta, he was a navigation system engineer at MITRE CAASD and a geodesist at Sidney B. Bowne and Son, LLP. He has a B.S. in civil engineering from the University of Miami and an M.S. in civil engineering from Purdue University.

R. Eric Phelts, Ph.D., is a research engineer in the Department of Aeronautics and Astronautics at Stanford University. He received his B.S. in Mechanical Engineering from Georgia Institute of Technology in 1995, and his M.S. and Ph.D. in Mechanical Engineering from Stanford University in 1997 and 2001, respectively. His research involves signal deformation monitoring techniques and analysis for SBAS and GBAS.

Todd Walter received his Ph.D. in Applied Physics from Stanford University in 1993. He is a Senior Research Engineer in the Department of Aeronautics and Astronautics at Stanford University. His research focuses on implementing high-integrity air navigation systems. He has received the ION Thurlow and Kepler awards. He is also a fellow of the ION and has served as its president.

Karl Kovach is a Senior Project Leader in the Navigation Division at The Aerospace Corporation in El Segundo, CA. Karl has been working on various aspects of the GPS program for over 37 years, including 3 years as the Air Force Officer-in-Charge of the GPS Control Segment when it was at Vandenberg AFB, CA (1983-1986). Karl received his B.S. degree in Mechanical Engineering from UCLA in 1978. He is a recipient of the ION Captain P.V.H. Weems award and the Satellite Division Johannes Kepler award.

Dr. Eric Altshuler received his B.S. in mathematics and computer science from UCLA in 1989 and his Ph.D. in physics in 1998 from University of California at Irvine. He is currently a Senior Software Engineer at Sequoia Research Company and is active in the development and implementation of ionospheric algorithms and prototyping for WAAS.

## ABSTRACT

The possibility of signal deformations on GPS signals has been a long standing threat requiring detection and mitigation with safety of life augmentation systems such as WAAS and GBAS. Numerous papers have been written on deformation monitoring and the threat model used to represent it. The propensity of signal deformation events to occur, however, can sometimes get lost since they are very rare. Over the passage of time, deformations have been observed on GPS and WAAS satellite signals and one of the purposes of this paper is to provide a list of known events and their characterization.

The deformation events that will be discussed are actual signal generation failures that occurred on GPS satellites, smaller deformations from satellite operations such as satellite power management and switching use of components, SVN 49 since it is a rather unique case of deformation, and lastly, a signal deformation event that was associated with WAAS GEO satellites. The WAAS GEO event occurred when two GEO signals were emanating from essentially the same point in space as one

satellite traversed from/to its intended orbital location. The paper will attempt, where possible, to describe the actual mechanism that caused these deformations.

The paper will also analyze one of the events to show the differential error possible from this satellite for a WAAS-corrected User for the entire class of allowed GPS equipment. Since aviation equipment allowed with WAAS and GBAS has a fairly large design space in terms of receiver correlator spacing and processing bandwidth, the relatively small errors observed with the WAAS and GBAS ground systems can be manifested as larger errors for a differentially corrected User.

## INTRODUCTION

The discovery of signal deformations on GPS signals was first documented with an event that occurred with SV19. In March 1993 at the Oshkosh Air Show, a pseudorange bias between C/A and P(Y) code measurements of approximately 4 m was observed with SV19 during aircraft landing experiments [1, 2]. Follow-on experiments also demonstrated that differential position accuracies, based on code pseudorange measurements, were less than 50 cm when SV19 was excluded but were on the order of several meters when this satellite was included. A signal anomaly on this satellite had been previously noted in constellation measurements conducted at Camp Parks Reserve Forces Training Area in Pleasanton, CA, but no action had been taken based largely on no user complaints or evidence of position degradation. The problem was resolved in January 1994 after the Operational Control Segment completed several corrective actions associated with using redundant signal transmission hardware. After the SV19 discovery, considerable focus by numerous organizations was directed at determining the source of the anomaly and ultimately it was concluded that a combination of analog-mode distortion and digital-mode timing error provided the most plausible explanation for all observations [2]. Since this discovery, signal deformations have evolved into a threat requiring detection and mitigation with safety of life augmentation systems such as WAAS and GBAS.

The primary purpose of this paper is to provide a list of signal deformation events and their characterization for GPS and WAAS L1 C/A signals. It is important to note that all transmitted C/A code signals have some level of deformation when compared with an ideal signal transmission and that this "nominal" deformation is not the concern of this paper. The interest of this paper is in discussing events where the shape of a satellite's C/A code correlation function was at a level where augmentation systems such as WAAS and GBAS precluded the satellite from being used or where a shift was observed when the satellite was healthy. The deformation events that will be discussed are actual signal generation failures that occurred on GPS satellites, smaller deformations from satellite operations such as satellite signal power management and switching use of components, SVN 49 since it is a rather unique case of deformation, and lastly, a signal deformation event that was associated with WAAS GEO satellites. For purposes of identifying and examining these events, the core source of information was generally from WAAS or GBAS reporting. A review of the fundamental processing used in WAAS for signal deformation monitoring (SDM) is provided in [3]. The deformation monitoring conducted in GBAS [4] also has very similar elements as those described for WAAS.

The other purposes of this paper are to examine some of these events and, to the extent possible, describe the actual failure mechanism(s) and also attempt to relate them to the signal deformation threat model. The threat parameter space for L1 C/A signal deformations is decomposed into an analog space essentially causing ripple on the code chip and digital space that relates the timing of chip edges. One example deformation event will be related to this threat representation and then analyzed to show how this deformation manifested itself in WAAS User equipment. Because WAAS ground station equipment and User equipment can use vastly different tracking and processing bandwidths, the signal deformation errors generally are not cancelled by differential correction. Therefore, some relatively modest pseudorange errors observed with the ground system can be seen as larger and significant errors for certain classes of User equipment.

## GPS DEFORMATION EVENTS

GPS deformation events discussed in this section cover two actual satellite failures, some deformations observed on IIR-M and IIF satellites associated with power management operations, and lastly, the SVN 49 implementation error that resulted in this satellite being unsuitable for use. The SVN 49 example is a rather unique case of deformation but it has been added for completeness.

### PRN 18 (SVN54, IIR) Deformation

The signal deformation with PRN 18 is one of the more interesting events because it occurred on two separate occasions and manifested itself in the exact same manner each time. The first occurrence in July 2009 lasted for 12 days while the second in March 2016 lasted for 60 days. Confirmation that the deformation was present and nearly constant over these two periods was determined through the WAAS Signal Quality Monitor (SQM), where the deformation was observed at 80 to 90% of the trip threshold. (The satellite is set Do not Use when the trip threshold is exceeded). The deformation being present for such long periods allowed for special data collection with a receiver that provides a direct measure of the satellite's C/A code chip (NovAtel ME3GG 3.0077D with Vision processing [5, 6]). The detailed sampling of the C/A code chip from this processing provides a more intuitive view of the deformation than the few sparse taps of the correlation function provided by WAAS or GBAS monitoring. Figure 1 shows the chip shape when the satellite was performing nominally (a) and in the deformed state (b). (Note: the convention in this paper is Figures on the left are "a" and those on the right are "b"). The data in these Figures are from both 2009 and 2016 and are remarkably similar for both nominal and deformed states. Notice also the deformed chip has additional ripple, indicative of some type of analog failure.

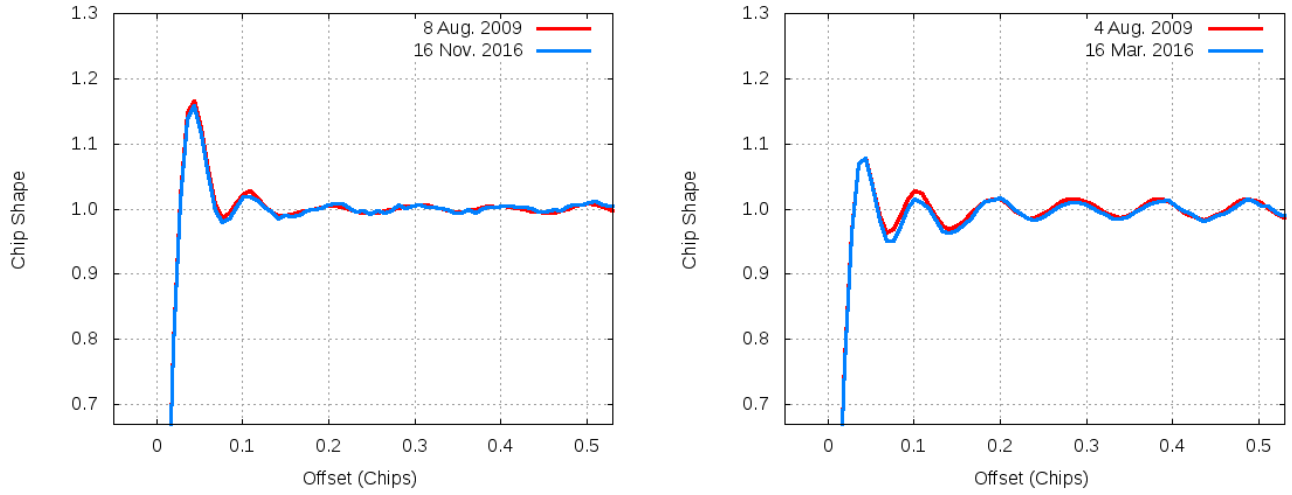


**Figure 1. PRN 18 chip shape comparisons from 2009 and 2016. (a) Shows PRN 18 with nominal performance and (b) shows deformed performance. Measurements were conducted with the same NovAtel receiver and WAAS reference station antenna from Zeta Associates Inc. (Fairfax, Virginia)**

The occurrence in 2009 was first noticed by GBAS when it started rejecting PRN 18 from its correction and integrity processing. A review of the event revealed the satellite was set unhealthy on 25 July and then set healthy the next day. On its first pass in view of the GBAS station, the satellite was rejected based on SDM exclusion. On 7 August, without any GPS operator intervention and while the satellite was set healthy, PRN 18 transitioned from this deformed state back to nominal. This transition occurred while the satellite was well viewed by the WAAS reference station in Honolulu and can be seen in Figure 2(a) as a shift in early correlator data approximately 6 hours 17 minutes into the GPS day. For presentation purposes, the correlator data measured at -0.1023 chip (green line) is biased positively by 0.055, at -0.0767 chip (red line) is biased by by 0.040, and at -0.05115 (purple line) is biased by 0.020. All measurements are normalized by prompt correlator value. Figure 2(b) also shows a shift of approximately 0.6 meter in L1 C/A pseudorange at this time. The measurements used to generate this Figure were processed by time aligning the previous sidereal day of code minus carrier corrected for ionosphere (CMCI) and differencing to minimize multipath. Interestingly, analysis of L2 pseudorange, L1 and L2 carrier, and L1 and L2 $C/N_0$ did not exhibit any change during this transition (or it was negligible). It should also be noted that the step in L1 pseudorange occurred over a very short time period, on the order of seconds.

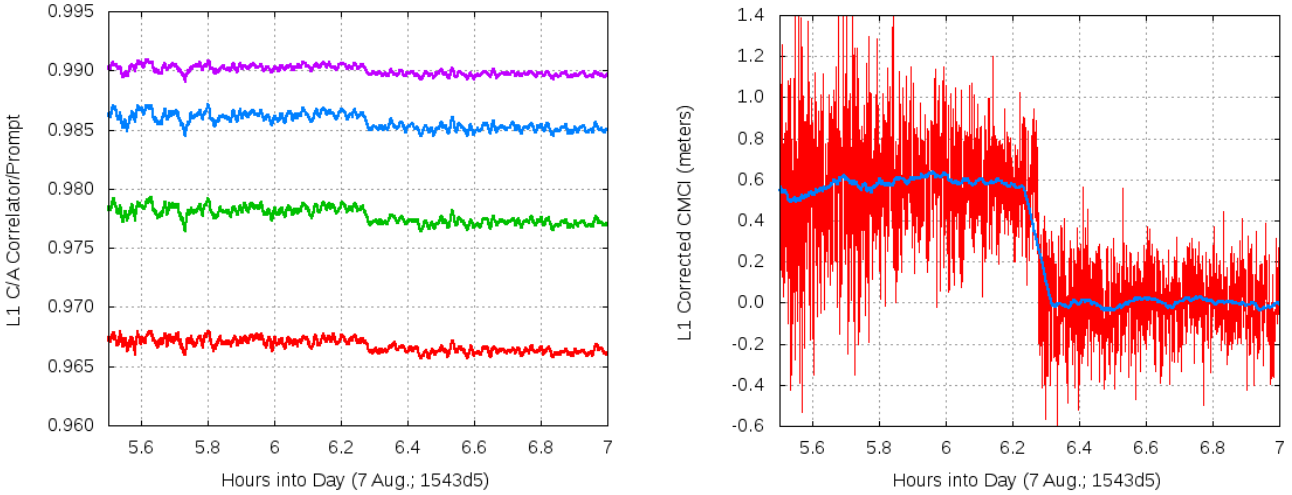


**Figure 2. PRN 18 transition from deformed to nominal on 7 August 2009 as observed from the Honolulu reference station. (a) Shows early L1 C/A correlator data normalized by prompt and (b) shows CMCI corrected for multipath.**

The PRN 18 signal deformation occurrence in 2016 was very similar to 2009. The satellite transitioned from the nominal state to the deformed state on 8 March and then back again on 7 or 8 May, while out of view of WAAS. For both transitions, the satellite was set healthy and GPS operations did not observe any deviation in their monitoring of satellite diagnostics. For the transition to the deformed state on the 8$^{th}$ of March the satellite was again well viewed by the Honolulu reference station and Figure 3 shows the same types of data discussed for the 2009 event transition. The transition to the deformed state occurred approximately 9 hours 22 minutes into the day as observed in both the correlator data and the L1 C/A pseudorange measurements. The pseudorange shift appears slightly larger this time, likely attributable to the wider 24 MHz processing bandwidth of the new WAAS G-III reference receiver versus the 18 MHz of the G-II receiver. Analysis of L2 pseudorange, L1 and L2 carrier and L1 and L2 $C/N_0$ again showed no change with this transition.

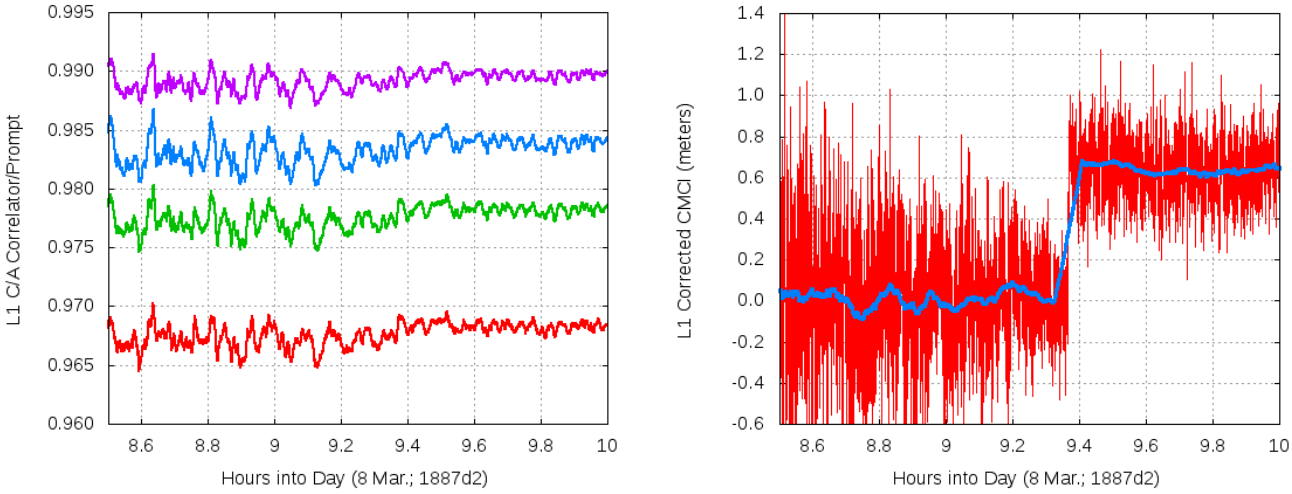


**Figure 3. PRN 18 transition from nominal to deformed on 8 March 2016 as observed from the Honolulu reference station. (a) Shows early L1 C/A correlator data normalized by prompt. (b) Shows CMCI corrected for multipath.**

The specific cause of the PRN 18 signal deformation has not been identified. It does appear to be associated with anomalous performance of some analog component in the L1 signal generation path based on the increased ripple on the L1 C/A code chip. As indicated above, the telemetry used to evaluate satellite performance and health did not show any unusual behavior at any of these transitions.

**PRN 02 (SVN61 IIR) Deformation**

PRN 02 experienced a signal deformation event on 31 October 2013 that again was first identified by GBAS as an SDM exclusion. The satellite continued to degrade until 3 November when it was set unhealthy and action was taken by GPS operators to switch to alternate signal generation hardware. To contrast onset of the event with its final anomalous state on 3 November, Figures 4 through 6 provide side-by-side comparisons of $C/N_0$, correlator measurements and L1 CMCI, respectively. The data in these Figures are from the WAAS reference station located at San José del Cabo in Mexico, which had good visibility for both the onset and when the satellite was finally set unhealthy. Figure 4(a) shows L1 and L2 $C/N_0$ and the failure can be seen in both measurements starting shortly after 15 hours into this day. In comparison, (b) shows $C/N_0$ on the 3rd where performance is degraded 4 or 5 dB for the majority of the satellite pass but there are intermittent times when the satellite transitions to performance that resembles nominal. (Interestingly, satellite performance appeared nominal during its pass on the 1st of November at San José del Cabo and again in this degraded state for the pass on the 2nd.) The satellite was finally set unhealthy on the 3rd of November approximately 17 hours into the day. Figure 5(a) shows early correlator data again with the onset clearly visible and then (b) where the correlator data can be seen shifted for most of the satellite pass. Lastly, Figure 6 shows L1 CMCI with pseudorange shifted up to approximately 2 meters during the periods of signal deformation. L1 and L2 carrier were investigated as well but other than increased noise due to reduced $C/N_0$ they were both well behaved during the onset and intermittent periods.

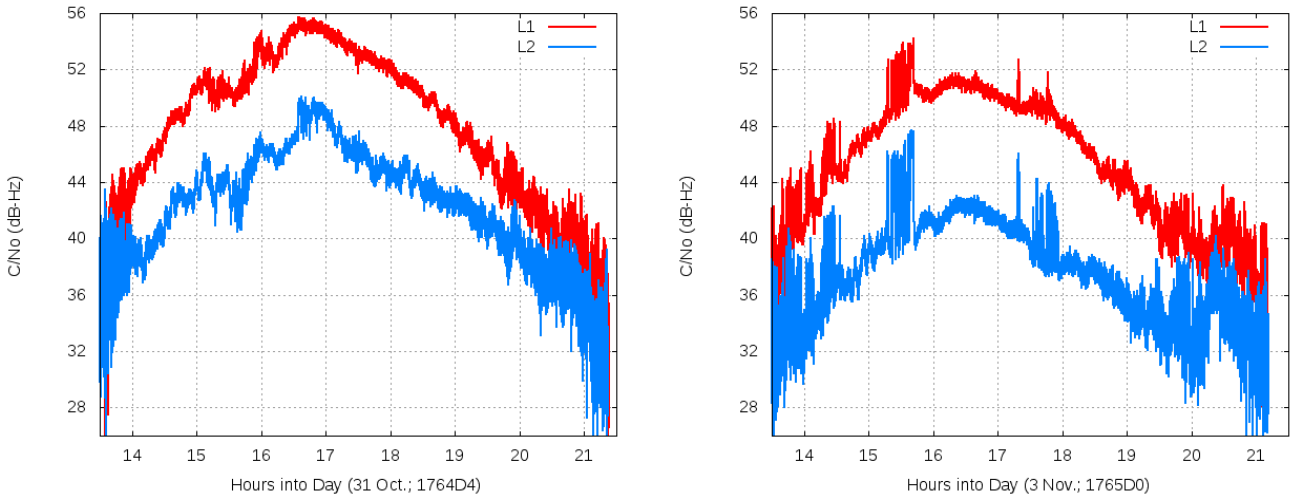


**Figure 4. PRN 02 $C/N_0$ observations from San José del Cabo reference station on (a) 31 October and (b) 3 November.**

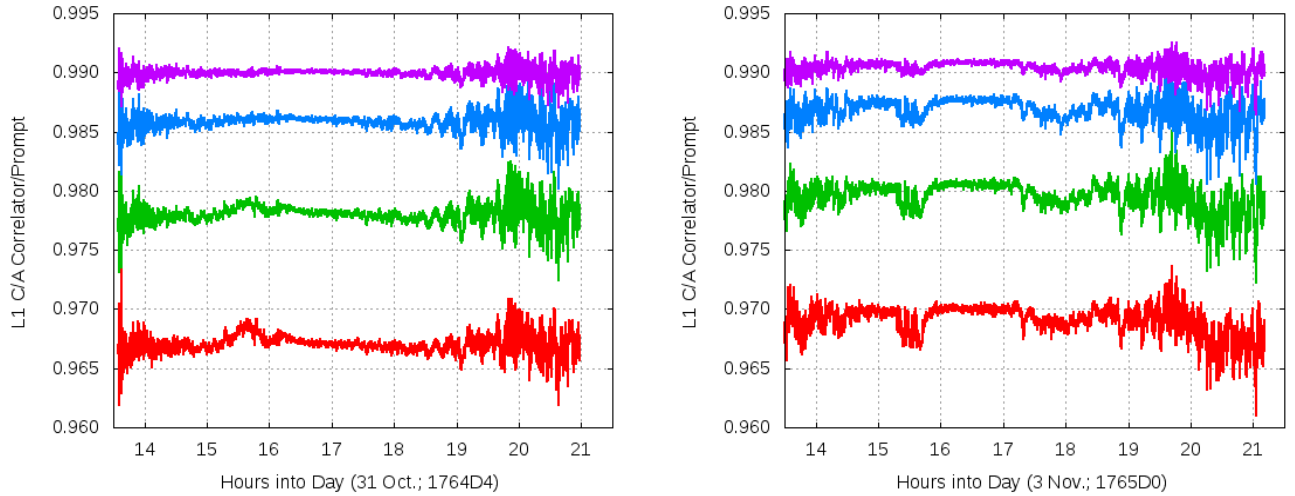


**Figure 5. PRN 02 correlator data from San José del Cabo reference station on (a) 31 October and (b) 3 November.**

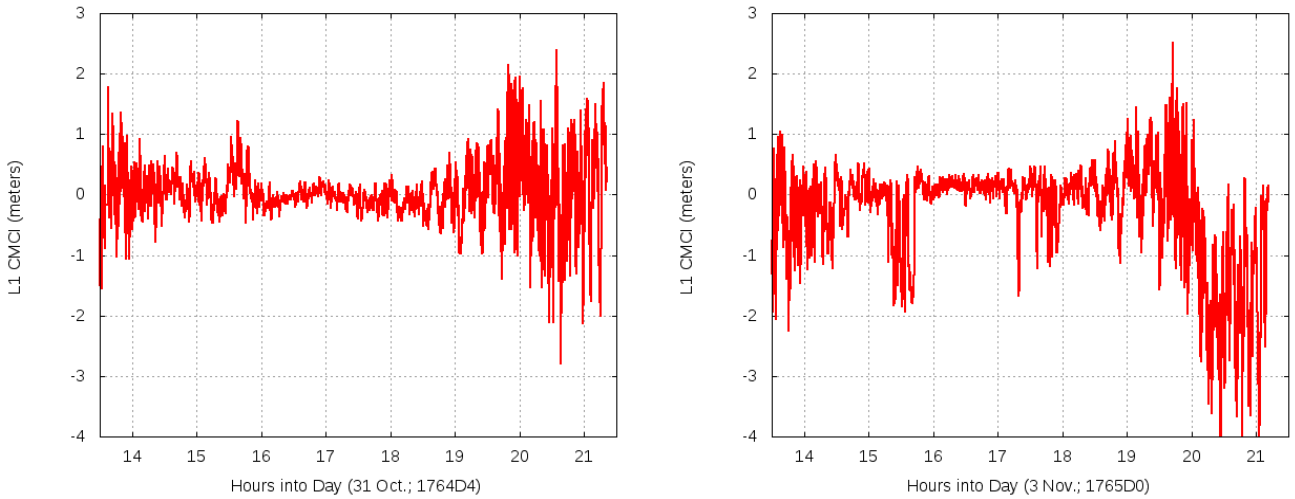


**Figure 6. PRN 02 L1 CMCI from San José del Cabo reference station on (a) 31 October and (b) 3 November.**

The cause of the PRN 02 anomaly was determined as a power failure that impacted satellite signal amplifiers in addition to other components. This particular failure mechanism is consistent with the observed degradation in L1 and L2 $C/N_0$. The reduction in gain presumably impacted passband group delay also, which led to correlator data deformation and ultimately pseudorange errors.

As mentioned above, the operators switched to an alternate signal path after the 3rd of November and the satellite was set healthy again on the 5th. As reported in [3], there was a small change in the nominal bias detected with this signal generation hardware switch, which is not unexpected. Figure 7(a) compares PRN 02 chip shapes from 2009 and 2016, which bridges this switch. For comparison purposes, Figure 7(b) compares PRN 16 chip shapes from the same time periods. While some elevation-dependent variation is expected from each satellite (see later discussion), these comparisons do appear to corroborate the nominal bias change for PRN 02.

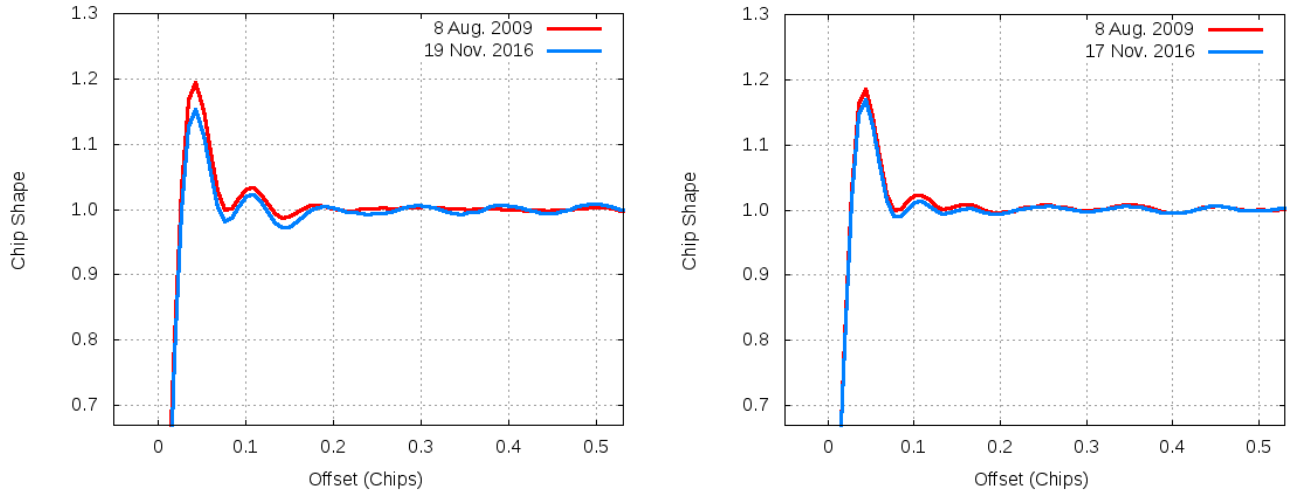


**Figure 7. Chip shape comparison from 2009 and 2016 for (a) PRN 02 and (b) PRN 16.**

**Power Management Operations (IIR-M & IIF Satellites)**

Starting with the IIR-M satellites, a capability was included where power could be adjusted onboard to different signals. In this discussion, we have looked at examples where P code power was increased ("High-P") as well as C/A power ("High-C/A"). The High-P capability has been observed on several occasions and is noticeable to the WAAS network in the L2 P(Y) $C/N_0$ estimates provided by the reference receiver. The first major campaign to demonstrate this capability on orbit was in September 2010, when all eight IIR-M's were tested, and a second concerted use was observed in July 2016. For the 2016

use of High-P, both IIR-M and IIF satellites were utilized. Figure 8(a) provides an example of L1 and L2 $C/N_0$ for PRN 12 during the July 2016 testing. The significant increase in L2 $C/N_0$ is when High-P presumably was commanded on this satellite. Figure 8(b) shows an un-normalized WAAS SQM detection metric for this same time period and the change in metric, while small, is clearly correlated with use of High-P. This change is likely on the order of the nominal bias shift discussed with PRN 02 above and has not presented any issues for WAAS or GBAS SDM.

The High-P testing in July 2016 involved eleven satellites over the course of three days (July 27th, July 28th and July 29th), each with different start and stop times and different durations. The WAAS SQM detection metrics used in SDM are normalized to lie between 0 and 1, and any that exceed 1 are considered faulted. The High-P testing had slight but measureable effects on the WAAS SQM metrics of all eleven satellites tested. To measure the percent of metric change, four baseline days were collected and a sidereal average for each metric was computed, i.e., the repeated metric trace of 86164 seconds was averaged to create a baseline trace. The times for the days in which the testing occurred for each PRN were aligned with the sidereal average, and differenced to create an absolute difference between the High-P time segment and the baseline time segment. An average was taken over the three days of testing, and the final values were multiplied by 100 to represent a "percentage of threshold" change in the SQM metrics. These values can be seen in Table 1 below. Notice the majority of detection metrics have small changes with High-P on the order of a few percent while just three metrics demonstrated a change of approximately 10%. The cause for the change in the L1 C/A correlation functions from High-P operation is not known.

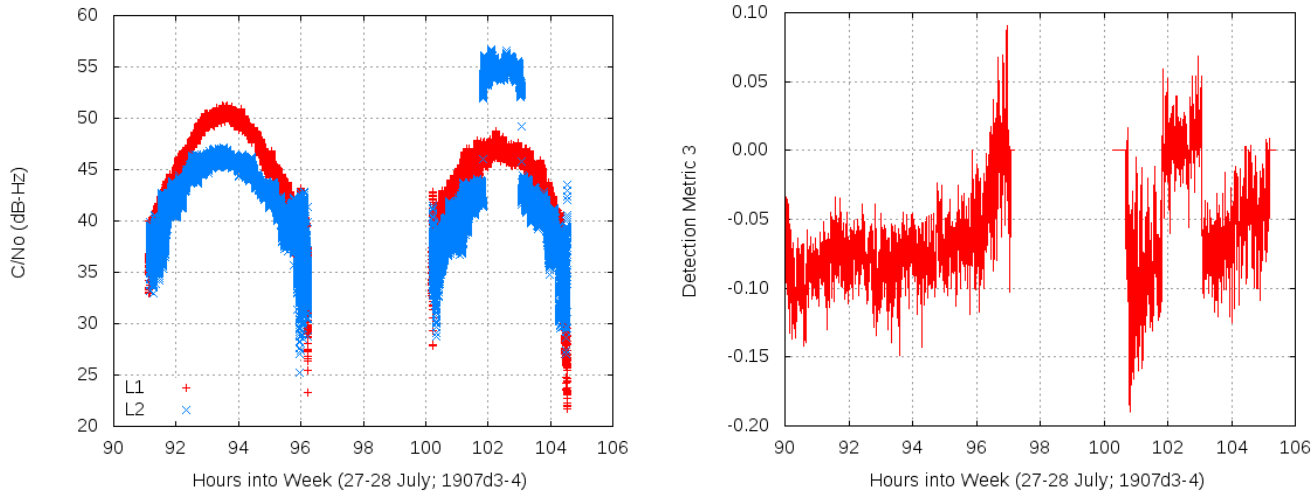


**Figure 8. PRN 12 during flex-power operations on 27-28 July 2016. (a) Compares L1 and L2 $C/N_0$ as measured from a WAAS reference receiver at Zeta. (b) Shows L1 C/A SQM Metric 3 responding to increase in L2 P(Y) signal power.**

**Table 1. High-P Operation Influence on WAAS SQM Detection Metrics per Satellite**

| Type | SVN | PRN | Metric 1 | Metric 2 | Metric 3 | Metric 4 |
|---|---|---|---|---|---|---|
| IIF | 63 | 1 | 1.53% | 2.42% | 2.78% | 3.28% |
| IIF | 69 | 3 | 2.43% | 0.78% | 6.40% | 1.68% |
| IIF | 72 | 8 | 1.79% | 1.76% | 2.12% | 1.93% |
| IIF | 73 | 10 | 2.15% | 1.00% | 2.71% | 3.87% |
| IIR-M | 58 | 12 | 5.56% | 1.27% | 9.75% | 3.17% |
| IIR-M | 55 | 15 | 2.55% | 2.77% | 3.88% | 1.69% |
| IIF | 65 | 24 | 2.48% | 2.18% | 5.50% | 2.16% |
| IIF | 62 | 25 | 3.18% | 4.21% | 1.61% | 3.45% |
| IIF | 66 | 27 | 3.76% | 4.89% | 10.23% | 5.41% |
| IIR-M | 52 | 31 | 4.33% | 1.84% | 7.16% | 4.71% |
| IIF | 70 | 32 | 6.97% | 1.41% | 11.03% | 7.33% |

Beginning 25 January 2017, a test effort was announced for IIR-M and IIF satellites (19 vehicles) to demonstrate the capability of increasing the L1 C/A power level. It was also reported in the test announcement [7] that High-C/A power would remain within IS-GPS-200-H specifications. The C/A power increase was implemented differently between satellite blocks where for IIR-M's the power was increased and remained at this level for the test period and for IIF's it was commanded once daily to the desired higher power level and then back to nominal power. The change in WAAS SQM detection metrics observed with High-C/A testing were generally comparable to that of High-P with the exception of one satellite pass for PRN 27 on the 28th which resulted in both an SDM exclusion with GBAS and trip with WAAS. Figure 9 shows PRN 27 L1 and L2 $C/N_0$ for a two hour period from four consecutive days when the satellite was near zenith for the Boston WAAS reference station. The days shown are the 26th through the 29th and GPS time has been adjusted appropriately for sidereal time to align data from 26–28 January with C/No data reported on the 29th (1934D0). The satellite pass on the 26th did not exhibit any satellite power management and is included to demonstrate nominal behavior while the 27th through the 29th had some power management. The day of interest is 28 January where instead of C/A power increasing it appears to have been inadvertently decreased and the same can be seen with L2 signal power. Figure 10(a) shows PRN 27 reference receiver early correlator data and 10(b) shows L1 CMCI for the same site and time period as the L1 and L2 $C/N_0$ shown in Figure 9. The distortion in the correlation function clearly aligns with the power reduction and the CMCI plot demonstrates this distortion resulted in a one meter change in L1 pseudorange. This PRN 27 event was the only significant SDM feature observed with this High-C/A testing and operators corrected the satellite configuration within one hour of its onset.

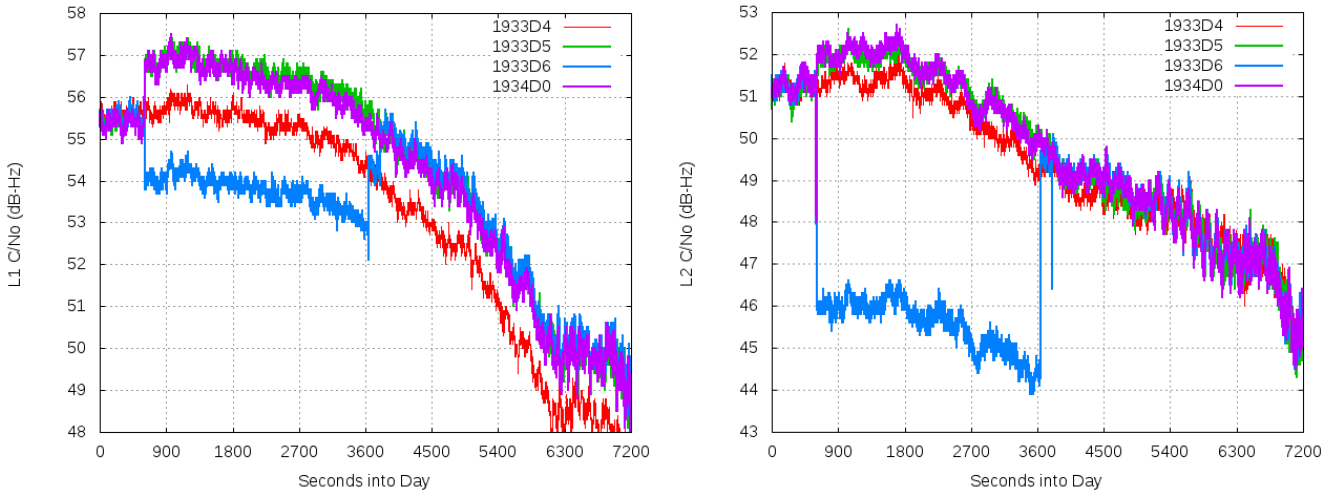


**Figure 9. PRN 27 during timeframe of High-C/A testing 26-29 January 2017. (a) Compares L1 $C/N_0$ and (b) compares L2 $C/N_0$ from a WAAS reference receiver at Boston.**

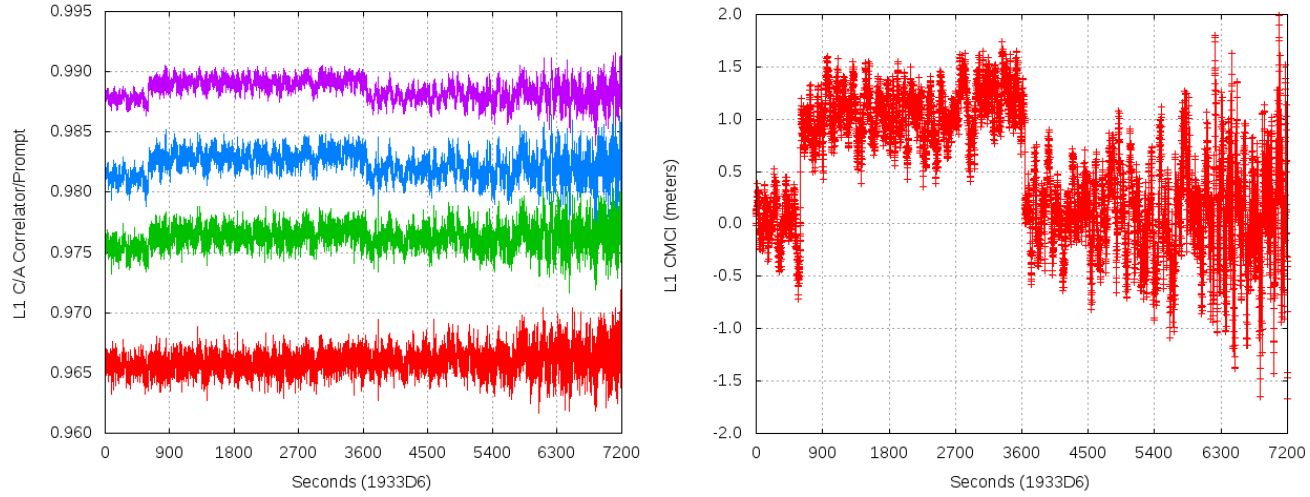


**Figure 10. PRN 27 observation from Boston reference station on January 28th. (a) Shows early L1 C/A correlator data normalized by prompt. (b) Shows L1 CMCI with a one meter change in range from the incorrect power setting.**

**PRN 01 (SVN49 IIR-M) Deformation**

Before it was launched, the GPS Block IIR-M satellite IIR-20M (also designated SVN49) underwent a critical modification in order to transmit an L5 signal in space from a GPS satellite by 26 August 2009, satisfying the requirement of an International Telecommunications Union filing to secure primary status of GPS in the L5 radiofrequency band. While the L5 Demo transmission from SVN49 was successful, soon after launch the U.S. Air Force reported "out-of-family" performance that prevented the satellite from being set healthy. Users worldwide with receivers capable of tracking the unhealthy satellite provided observations of L1 and ionosphere-free pseudorange showing varying elevation-dependent measurement biases. The root cause ultimately was determined to be leakage of the primary L1/L2 signal through the power divider of the antenna array and reflection due to impedance mismatch at the L5 bandpass filter, with the return signal then broadcast through the transmit antenna. Such performance manifests much like signal multipath and, as such, receivers with different tracking technology are affected by different elevation-dependent measurement errors [8].

Figure 11 compares the C/A code chip shape for PRN 01 (SVN49) with that of PRN 30 (SVN30, which had a ground track nearly identical to SVN49 at the time so it was useful for data collection and performance comparison). The data for the plots in Figure 11 came from the NovAtel receiver equipped with Vision processing, mentioned previously. The different colored lines show chip shape estimates for different elevation angles. Note how the shape for PRN 01 exhibits significant variation whereas the shape for PRN 30 is largely uniform over the range of elevation angles. The variation signature for PRN 01 shows distortions centered at approximately 0.04 and 0.08 chip offset (~ 12 and 24 m), indicative of multipath signals with corresponding delays.

Figure 12 compares the resultant errors on L1 C/A narrow correlator pseudorange measurements by elevation angle for PRN 01 and PRN 30, along with similar error signature plots for L2 P(Y) semi-codeless measurements. It is clear significant biases by elevation angle exist for PRN 01 while the signatures for PRN 30 are as flat as would be expected for typical pseudorange measurements. Note there have been reports of elevation-dependent distortions on other GPS satellites [9] but the effects are not nearly as severe as those for SVN49, which continues to be set unhealthy to this day because of them.

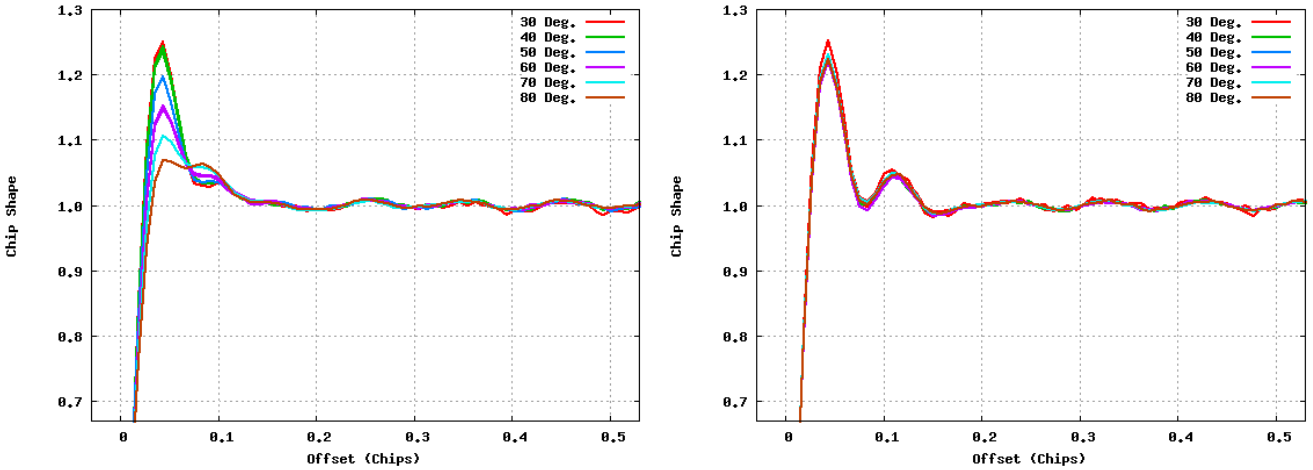


**Figure 11. L1 C/A chip shape measured for specific elevation angles (a) for PRN 01 and (b) for PRN 30.**

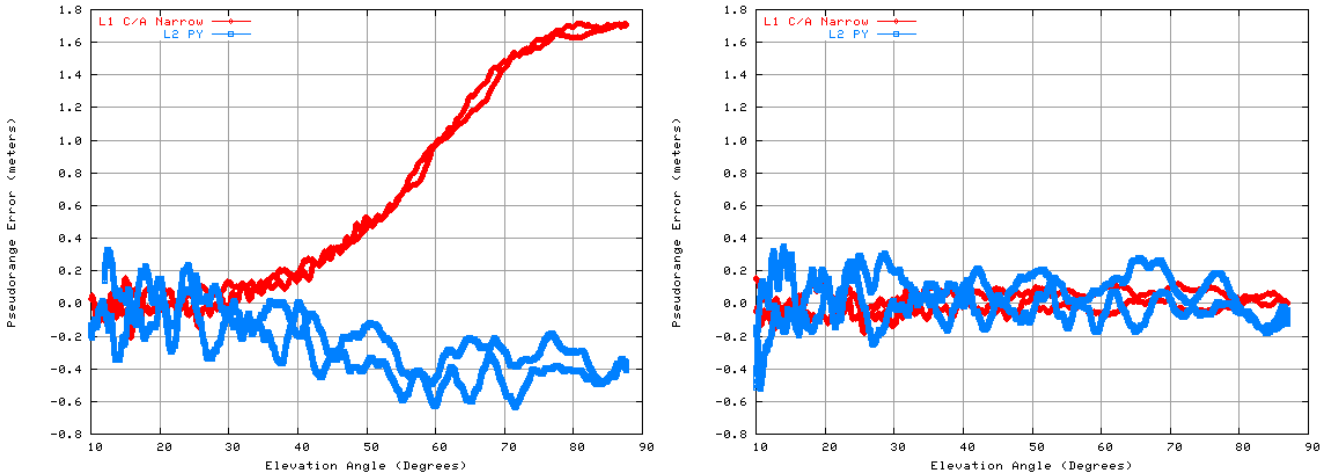


**Figure 12. L1 C/A and L2 P(Y) Semi-codeless CMCI versus elevation angle for PRN 01 (a) and for PRN 30 (b)**

## WAAS DEFORMATION EVENT

Galaxy 15 (CRW) is a GEO satellite used by WAAS that experienced a failure in April 2010, resulting in loss of all telemetry and control to this satellite. As a result, the satellite drifted from its assigned orbital location of 133W to 97W over the course of a nine-month period. In December 2010, autonomous attitude control by CRW could no longer be maintained and this resulted in loss of sun orientation and then satellite power. After the satellite became re-oriented it reset, which allowed recovery of communications and control. CRW was then maneuvered back to a location close to its original orbital slot. WAAS maintained a ranging signal from this satellite throughout most of this period although integrity bounds associated with this signal were degraded as it moved away from its nominal orbital location [10].

During the course of this satellite's drift it encountered another WAAS satellite (CRE) at 107.3W where for brief periods they were both emanating from essentially the same point in space. The first occurrence was the 11$^{th}$ through the 13$^{th}$ of November 2010, during which the CRW satellite's orbit was not controlled, and the second was on the 3$^{rd}$ of March 2011 as CRW was being maneuvered back toward its original orbital location. In both instances, when the pointing difference between the satellites was less than a quarter degree in azimuth and elevation, an increase in WAAS SQM metrics was observed and in March the monitor actually tripped, setting the satellites "Do Not Use". Figure 13(a) highlights the first interaction, showing L1 C/A $C/N_0$ as measured by the dish antennas of the stations controlling these GEOs (Napa was the WAAS uplink site controlling CRW and Brewster controlling CRE) and Figure 13(b) shows the variation in the correlator positioned at -0.05115 normalized by prompt. As a reminder, WAAS signals are generated on the ground and signal transmitted via C-band uplinks to each GEO where the signal is downconverted to the L1 frequency. The uplinks in this case were separated by approximately 14 MHz and each signal is bandlimited at the signal generator to approximately 22 MHz. This results in C/A code signals on these uplinks overlapping at each GEO satellite by approximately 8 MHz.

Figure 14(a) shows an expanded view of the correlator variation for CRW and Figure 14(b) for CRE. Also shown in these Figures are correlator variations observed with a WAAS reference receiver at Zeta Associates in Fairfax, Virginia. Notice the behavior is very structured and highly correlated with measurements from Zeta. This observation was confirmed with other WAAS reference station measurements and indicates the source of the variation was from the satellite. (Note: correlator data available directly from the signal generation equipment at the uplink sites confirmed the variation was not being generated by the ground equipment.) An additional observation shown in these Figures involves the times when the difference between geometric ranges to CRW and CRE is exactly modulo 293 meters (1 chip) from either Napa or Brewster. For example, the variation in correlator data observed on the CRW signal is correlated with the range difference to these satellites as computed from the uplink site controlling CRE. This observation is further demonstrated in Figures 15(a) and 15(b) by computing the period of the dominant correlator feature with the code alignment period described above.

Figures 16 through 18 show the same data from the second crossing in March 2011. The results are very much the same as November despite the interactions between the two WAAS GEOs being very different. The root cause of the signal deformation, while somehow associated with chip alignment, is still not understood.

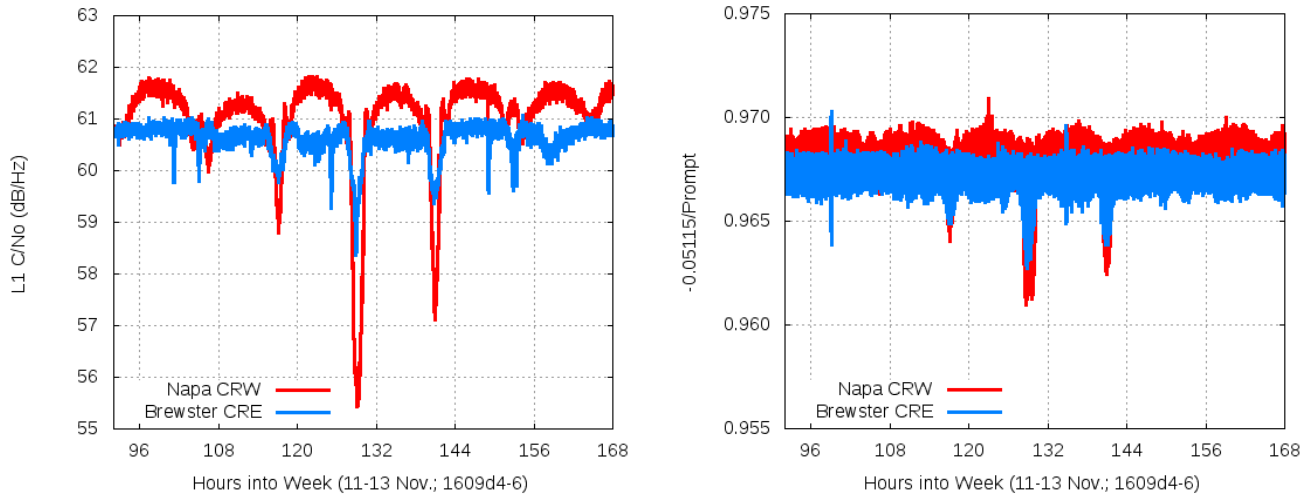


**Figure 13. Comparison of $C/N_0$ from downlink antennas (a) and correlator measurements (b, -0.05115/Prompt)**

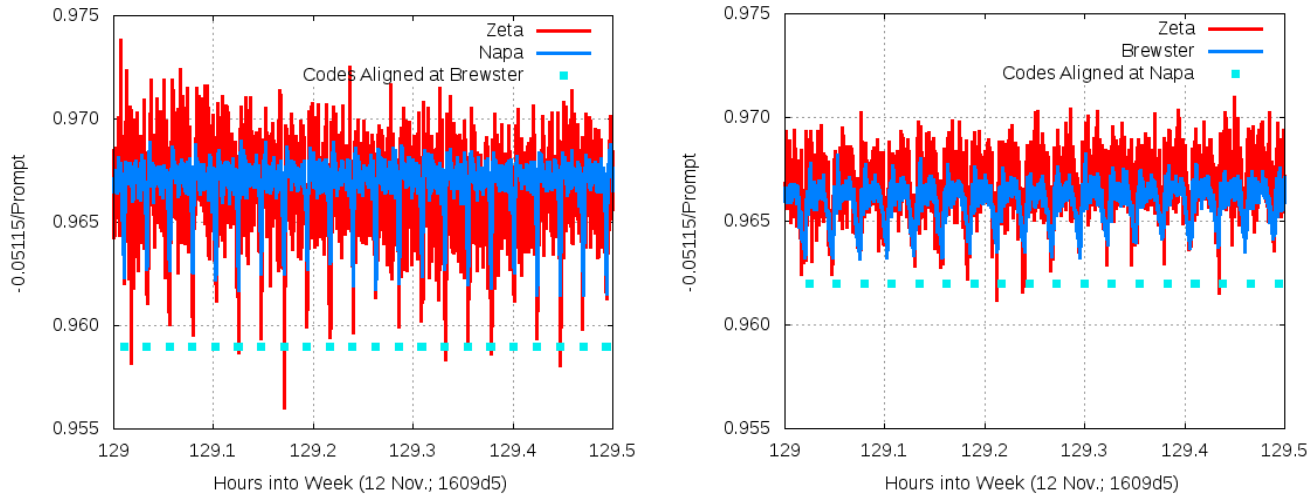


**Figure 14. Expanded view of correlator data from downlink antennas and measured at Zeta. (a) Shows CRW with code aligned periods computed at Brewster. (b) Shows CRE with code aligned periods computed at Napa.**

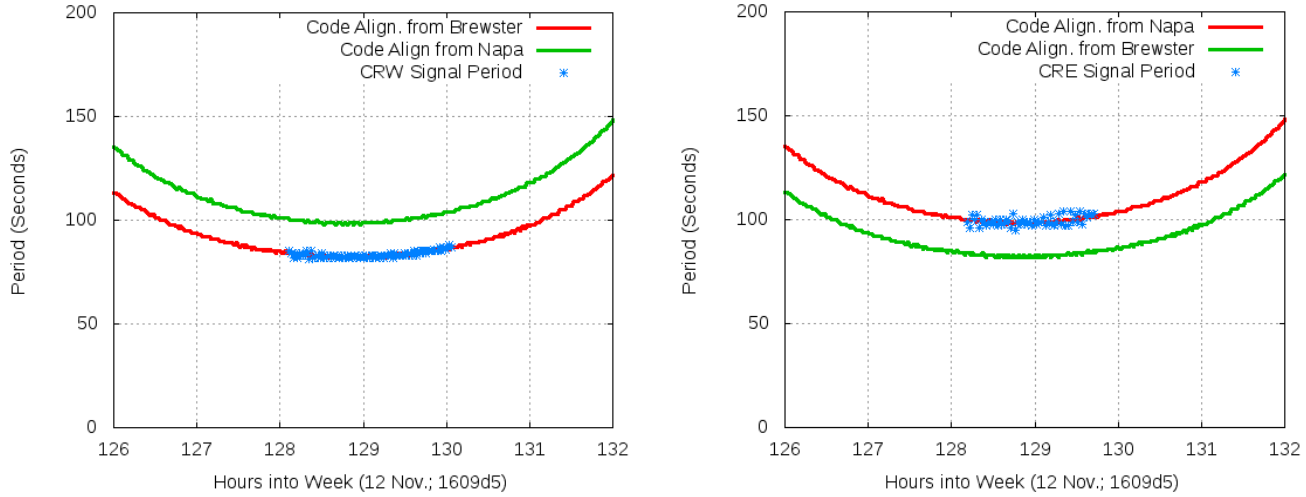


**Figure 15. Comparison of code alignment and correlator variation periods. (a) Shows CRW signal variation matches code alignment from Brewster. (b) Shows CRE signal variation matches code alignment from Napa.**

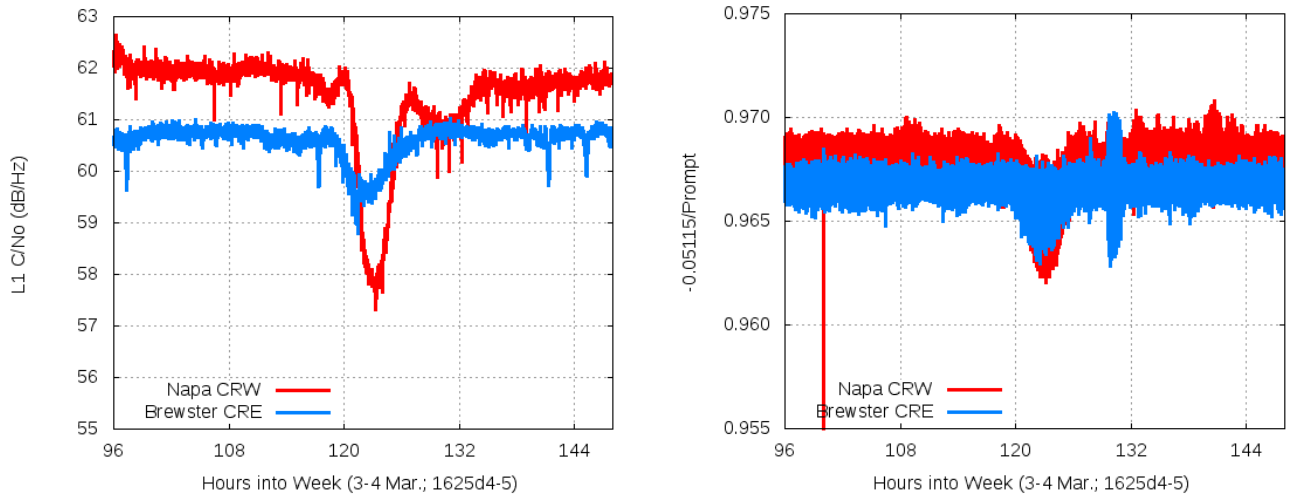


**Figure 16. Comparison of $C/N_0$ from downlink antennas (a) and correlator measurements (b, -0.5115/Prompt)**

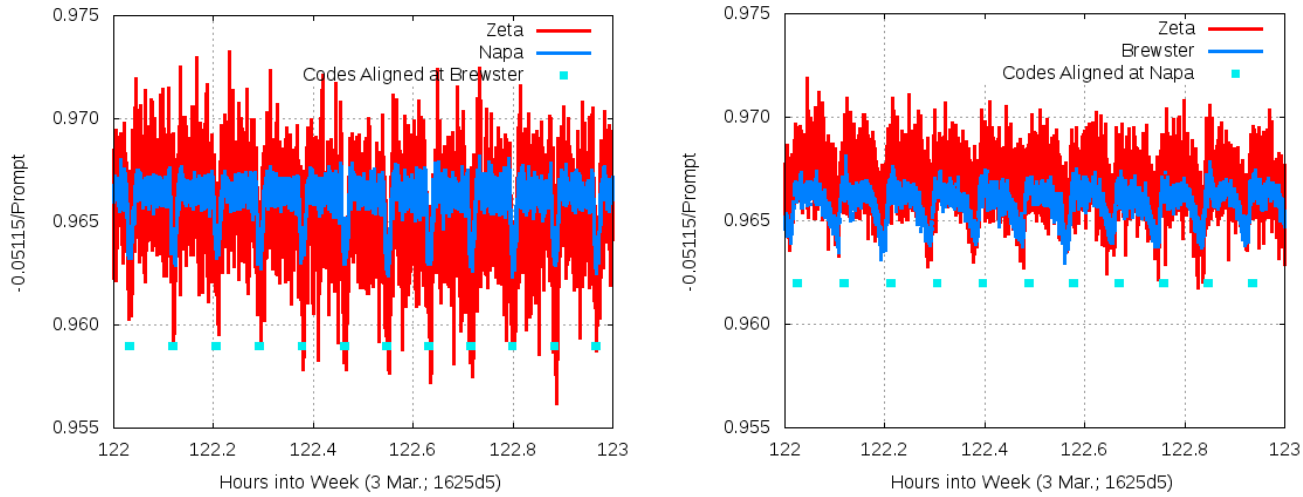


**Figure 17. Expanded view of correlator data from downlink antennas and measured at Zeta. (a) Shows CRW with code aligned periods computed at Brewster. (b) Shows CRE with code aligned periods computed at Napa.**

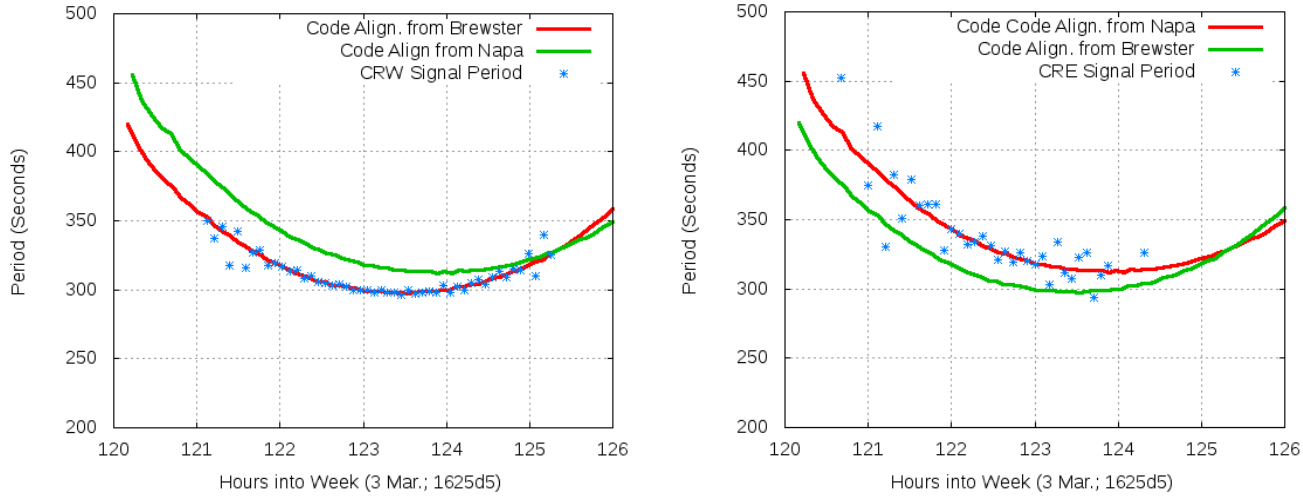


**Figure 18. Comparison of code alignment and correlator variation periods. (a) Shows CRW signal variation matches code alignment from Brewster. (b) Shows CRE signal variation matches code alignment from Napa.**

## ASSESSING FAILURES VS. DEFORMATION THREAT MODEL

Using the code chip shape data recorded from the NovAtel receiver for PRN 18 shown earlier, the signal deformation was analyzed to assess how it would manifest itself in WAAS User equipment. Because WAAS ground station equipment and User equipment can use vastly different tracking and processing bandwidths, the signal deformation errors generally are not fully differentially corrected. Therefore, some relatively modest pseudorange errors observed with the ground system can correspond to larger and more significant errors for certain classes of User equipment.

Figure 19 shows the chip shapes and corresponding correlation peaks for PRN 18 compared to 15 other satellites tracked by the same receiver. PRN 18 stands out in both the chip and correlation domains. Both the analog oscillations of its chip shape and the amplitude of the correlation peak are noticeably smaller than those of the other signals. The median chip shape (and peak) is also plotted since WAAS uses this metric as its reference from which the others are individually measured [3]. That applies for both monitoring and for estimation of the user range errors.

A comparison of the nominal vs faulted user errors for a range of User receiver bandwidths and correlator spacings is provided in Figure 20. (The current allowed receiver filter/discriminator configurations are outlined in black boxes.) While all the modeled nominal errors remain below 50 cm for all User receiver configurations when there is no fault, the largest user error approximately doubles when PRN 18 becomes distorted. While this may not seem significant compared to current user range error limits for WAAS, for dual-frequency errors this would be unacceptable [11]. (Figure 20 also shows how the proposed reduction to allowable receiver configurations would mitigate this potential threat.) The analog and digital threat model parameters corresponding to this type of signal deformation (and that of SVN49) are examined in [12].

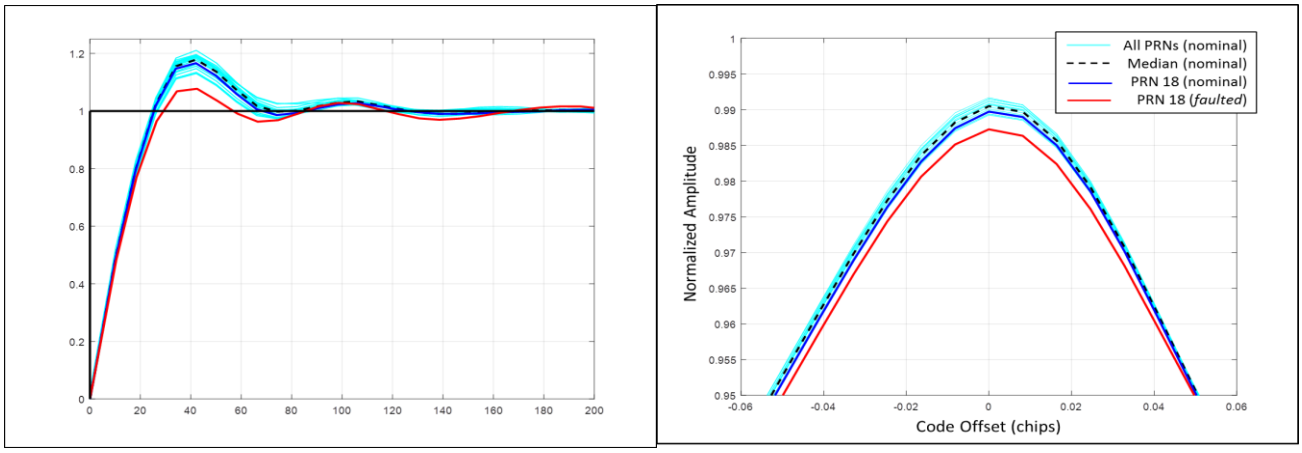


**Figure 19. PRN 18 deformed and nominal chip shape (a) and correlation function modeling (b)**

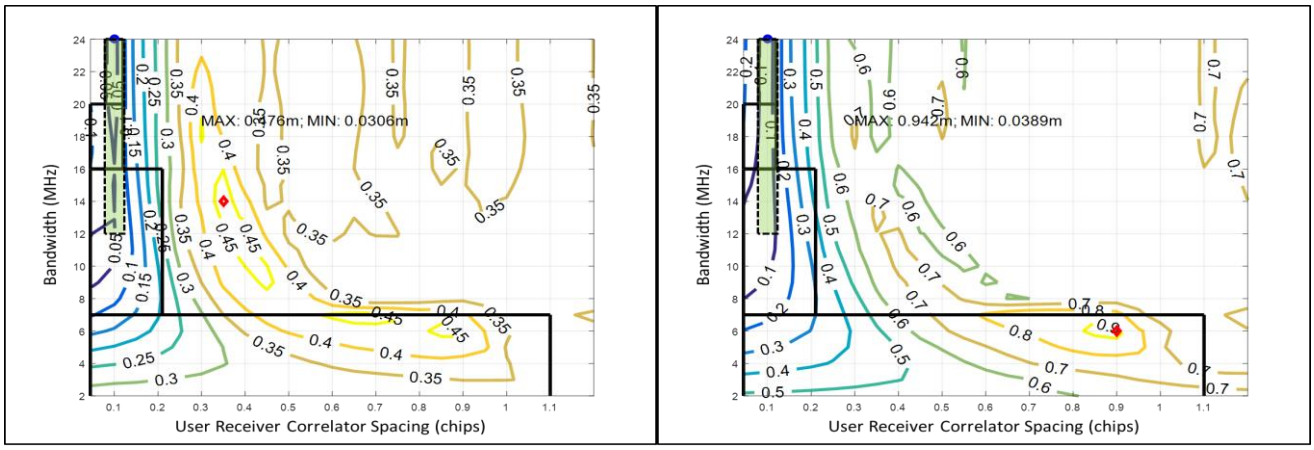


**Figure 20. Early-Minus-Late User no fault case for PRN 18 (a) and faulted case (b). (Green shaded region denotes proposed allowed receiver configurations for future dual-frequency WAAS users.)**

## SUMMARY

The L1 C/A signal deformation threat now has a long and established standing that must be mitigated in safety critical systems. SV19 was the foundational event for signal deformations and this paper has documented other events that have occurred since. The deformation events discussed were actual signal generation failures that occurred on GPS satellites, deformations from satellite operations such as satellite power management and switching use of components, SVN 49 and its elevation dependent range biases, and lastly, a signal deformation event that was associated with WAAS GEO satellites.

An important realization in developing this paper is the maturity of the highly sensitive and capable monitoring capabilities for signal deformations that now exist in augmentation systems. The techniques developed and implemented in WAAS and GBAS provide tremendous insight into the slightest perturbations in the L1 C/A correlation functions. This same monitoring capability will now need to be extended to the L5 signal as well as augmentations systems intending to monitor and correct other GNSS signals.

## ACKNOWLEDGMENTS

The authors would like to acknowledge that this effort was sponsored by the FAA GNSS program office. The authors would also like to acknowledge and thank Dr. Per Enge from Stanford University for partially motivating this paper through his significant contributions to the signal deformation area as well as his somewhat creative counting of observed events.

## REFERENCES

[1] Edgar C, Czopek F, Barker B, “A co-operative anomaly resolution of PRN-19”, ION GPS 1999

[2] Mitelman A.M., “Signal Quality Monitoring For GPS Augmentation Systems”, Ph.D. Thesis (2005), Stanford University, Stanford, CA

[3] Phelts R.E., Altshuler E, Walter T, Enge P, “Validating Nominal Bias Error Limits Using 4 years of WAAS Signal Quality Monitoring Data”, ION Pacific PNT 2015

[4] Liu, F, Brenner, M, Tang, C.Y., "Signal Deformation Monitoring Scheme Implemented in a Prototype Local Area Augmentation System Ground Installation", ION GNSS 2006

[5] Weill L.R., “Theory and Applications of Signal Compression in GNSS Receivers”, ION GNSS 2007

[6] Fenton P, Jones J, “The Theory and Performance of NovAtel Inc.’s Vision Correlator”, ION GNSS 2005

[7] U.S. Coast Guard, “Limited Duration GPS C/A Power Testing”, January, 25th, 2017

[8] Ericson S, Shallberg K, Edgar C, “Characterization and Simulation of SVN49 (PRN01) Elevation Dependent Measurement Biases”, ITM 2010

[9] Springer T, Dilssner F, “SVN49 and Other GPS Anomalies”, Inside GNSS July/August 2009

[10] Shallberg K, Potter B.J., Class P, “Geostationary Satellite Reference Station Multipath Characterization: Using Galaxy 15 Failure to Refine the WAAS Multipath Threat”, ION GNSS 2011

[11] Phelts R.E., Wong G, Walter T, Enge P, "Signal Deformation Monitoring for Dual-Frequency WAAS", ITM 2013

[12] Phelts R.E., Shallberg, K, Walter T, Enge P, “WAAS Signal Deformation Monitor Performance: Beyond the ICAO Threat Model”, ION Pacific PNT 2017